

Thermophysical Properties of the Equimolar Mixture $\text{NaNO}_3\text{-KNO}_3$ from 300-600°C

D. A. Nissen

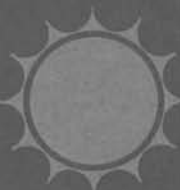
Prepared by Sandia National Laboratories, Albuquerque, New Mexico 87185 and Livermore, California 94550 for the United States Department of Energy under Contract DE-AC04-76DP00789.

Printed November 1980

When printing a copy of any digitized SAND Report, you are required to update the markings to current standards.



Sandia Laboratories
energy report



Issued by Sandia National Laboratories, operated for the United States
Department of Energy by Sandia Corporation.

NOTICE

This report was prepared as an account of work sponsored by the United States Government. Neither the United States nor the United States Department of Energy, nor any of their employees, makes any warranty, express or implied, or assumes any legal liability to responsibility for the accuracy, completeness or usefulness of any information, apparatus, product or process disclosed, or represents that its use would not infringe privately owned rights.

Printed in the United States of America
Available from
National Technical Information Service
U. S. Department of Commerce
5285 Port Royal Road
Springfield, VA 22161
Price: Printed Copy \$4.00; Microfiche \$3.00

THERMOPHYSICAL PROPERTIES OF THE EQUIMOLAR
MIXTURE $\text{NaNO}_3\text{-KNO}_3$ FROM 300-600°C

D. A. Nissen
Exploratory Chemistry Division I
Sandia National Laboratories, Livermore

ABSTRACT

The thermophysical properties (viscosity, surface tension, and density) of the molten equimolar mixture $\text{NaNO}_3\text{-KNO}_3$ have been determined over the temperature range 300-600°C in argon and in oxygen. The surface tension is a linear function of the temperature and can be represented by the expression

$$\gamma(\text{dynes/cm}) = 133.12 - 6.25 \times 10^{-2}T(\text{°C}) .$$

The viscosity may be calculated from the equation

$$\eta(\text{cP}) = 22.714 - 0.120T + 2.281 \times 10^{-4}T^2 - 1.474 \times 10^{-7}T^3 ,$$

for T in °C, with an uncertainty of 1.0%. The viscosity can be characterized by two activation energies. For temperatures below 385°C, $E_\eta = 4.5 \text{ kcal/mole}$; above 385°C, $E_\eta = 3.2 \text{ kcal/mole}$, in argon and in oxygen. This suggests that at temperatures below 385°C free rotation of the nitrate ion becomes restricted, with a consequent increase in the activation energy for viscous flow. In argon the density is given by

$$\rho(\text{g/cm}^3) = 2.090 - 6.36 \times 10^{-4}T(\text{°C}) .$$

However, if the melt is held at 600°C, for extended periods the density begins to decrease slowly due to formations of nitrite. After 72 hours at 600°C the density is given by

$$\rho(\text{g/cm}^3) = 2.062 - 6.11 \times 10^{-4}T(\text{°C}) .$$

THERMOPHYSICAL PROPERTIES OF THE EQUIMOLAR MIXTURE $\text{NaNO}_3\text{-KNO}_3$ FROM 300-600°C

Introduction

The equimolar molten salt mixture $\text{NaNO}_3\text{-KNO}_3$ is being proposed as a heat-transfer fluid and thermal-energy storage medium for various solar energy applications. In these applications the maximum operating temperature will be in the range 500-600°C. Industrial experience and previous experimental investigations on this molten salt mixture have generally been confined to temperatures below 450°C. In order to provide data to solve various specific design problems associated with the use of these molten nitrate salts as heat transfer fluids, it is important that we know how the physical properties of these salts are affected by temperature and composition of the liquid and gas phases. It is the purpose of this report to present and comment on the viscosity, surface tension, and density data we have measured over the temperature range 300-600°C.

Apparatus and Experimental Technique

The thermophysical property data for the equimolar $\text{NaNO}_3\text{-KNO}_3$ mixture were taken by an instrument designed and built by the author at SNLL.¹ This instrument is based on the principle of a damped, one-dimensional, harmonic oscillator, i.e., the motion of a body suspended from a spring and oscillating in a fluid. A description of the theoretical principles which govern the operation of this instrument, the details of construction, and its operation and response are discussed elsewhere.¹ Only an abbreviated description of the various modes of operation of this instrument will be given here.

The heart of the apparatus is a quartz spring oscillator, an electromagnet for remotely starting the spring oscillating, a position transducer for remote readout of the spring extension (linear variable differential transformer--LVDT), and a gold plate suspended in a liquid whose viscosity is being measured (see Figure 1). It is the viscous drag exerted on this plate by the liquid which causes damping of the oscillatory motion of the quartz spring.

The liquid being studied is contained in a gold crucible mounted on a pedestal fastened to a screw and yoke arrangement.* This is attached to the bottom flange of an intermediate quartz tube. The pedestal and screw are

*For simplicity only the screw is shown in Figure 1; however, Figure 2 shows the yoke clearly.

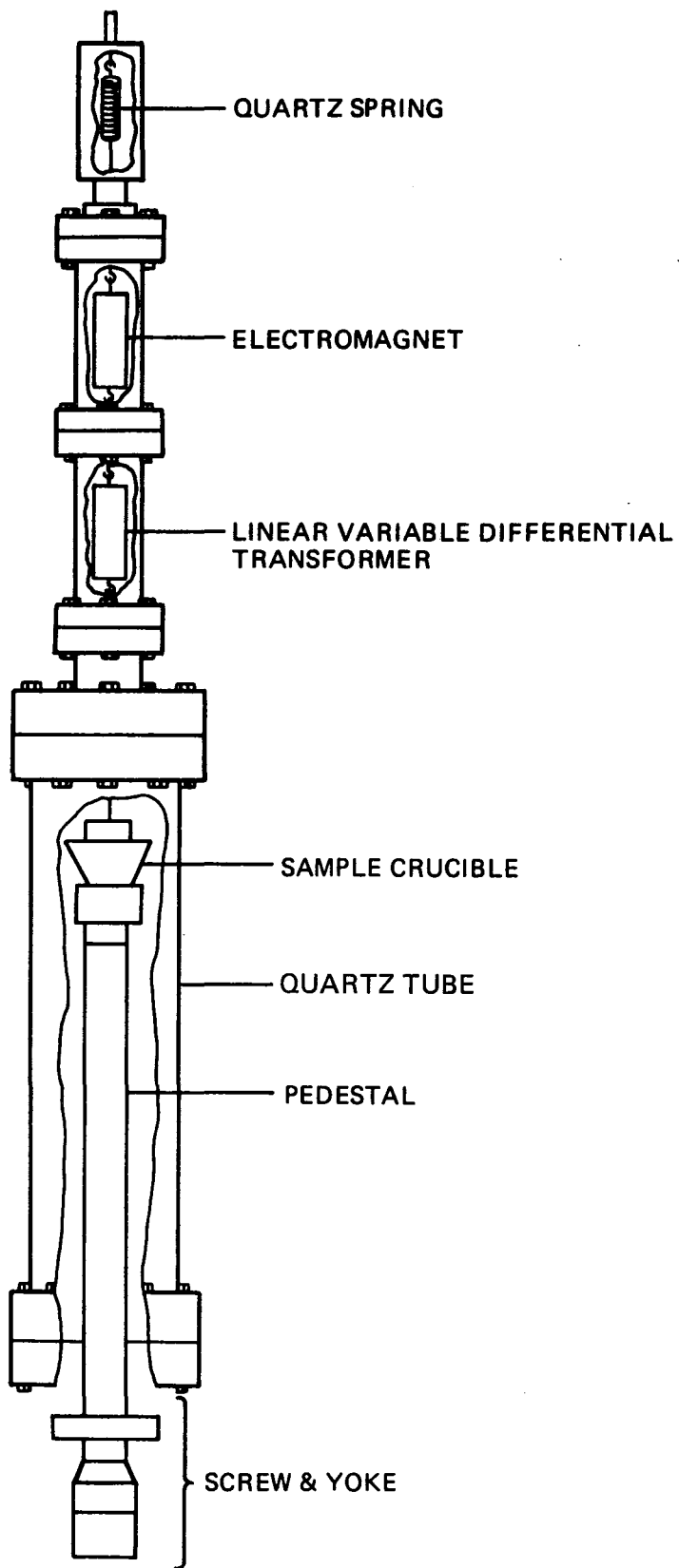


Figure 1. Viscometer Assembly (cutaway)

connected by a machined stainless steel rod which passes through a compression fitting designed to maintain the integrity of the atmosphere within the viscometer. This arrangement permits the crucible and its contents to be raised or lowered smoothly and slowly about 4 cm. It is the ability to lower the crucible which is central to the surface tension measurement, as will be clear from later discussion.

A thermocouple sheathed in stainless steel is fed through a fitting in the bottom flange and bent to allow its tip to be immersed in the liquid. In this way the temperature of the liquid can be monitored continuously. A gold sheath on the tip of the thermocouple prevents any reaction between it and the liquid. The bottom flange also has a tube welded into it for admitting gas into the heated zone.

A clam-shell-type furnace, mounted on the supporting structure, is fastened around the quartz tube to heat the contents of the crucible (Figure 2). This furnace and its associated controller are capable of maintaining the temperature of the crucible contents to within $\pm 0.5^{\circ}\text{C}$ of the set point. The vertical temperature gradient over the 5 cm height of the crucible is $< 1^{\circ}\text{C}$.

Viscosity

It is possible to show² that for a damped harmonic oscillator the ratio of any arbitrary zeroth oscillation to the nth successive one is given by

$$\frac{y_0}{y_n} = e^{2\pi np} \\ = e^{n\delta} \quad (1)$$

where p is a constant. The quantity δ , known as the logarithmic decrement, is given by

$$\delta = \frac{1}{n} \ln \frac{y_0}{y_n} \quad (2)$$

and is therefore a measure of the rate of damping of the oscillations of the spring. Solomons and White³ have shown that δ is directly related to the viscosity of the damping medium by the equation

$$\sqrt{np} = D\delta - E \quad (3)$$

where n and p are the viscosity and density of the liquid being studied. Both D and E are instrument constants:

The constants D and E were evaluated by measuring δ for molten KNO_3 , whose viscosity and density are well known,⁴ and for a set of specially prepared organic liquids whose viscosity and density are accurately known. These liquids, supplied by Cannon Instrument Co., have a viscosity range of 1.5-5.0 cP.

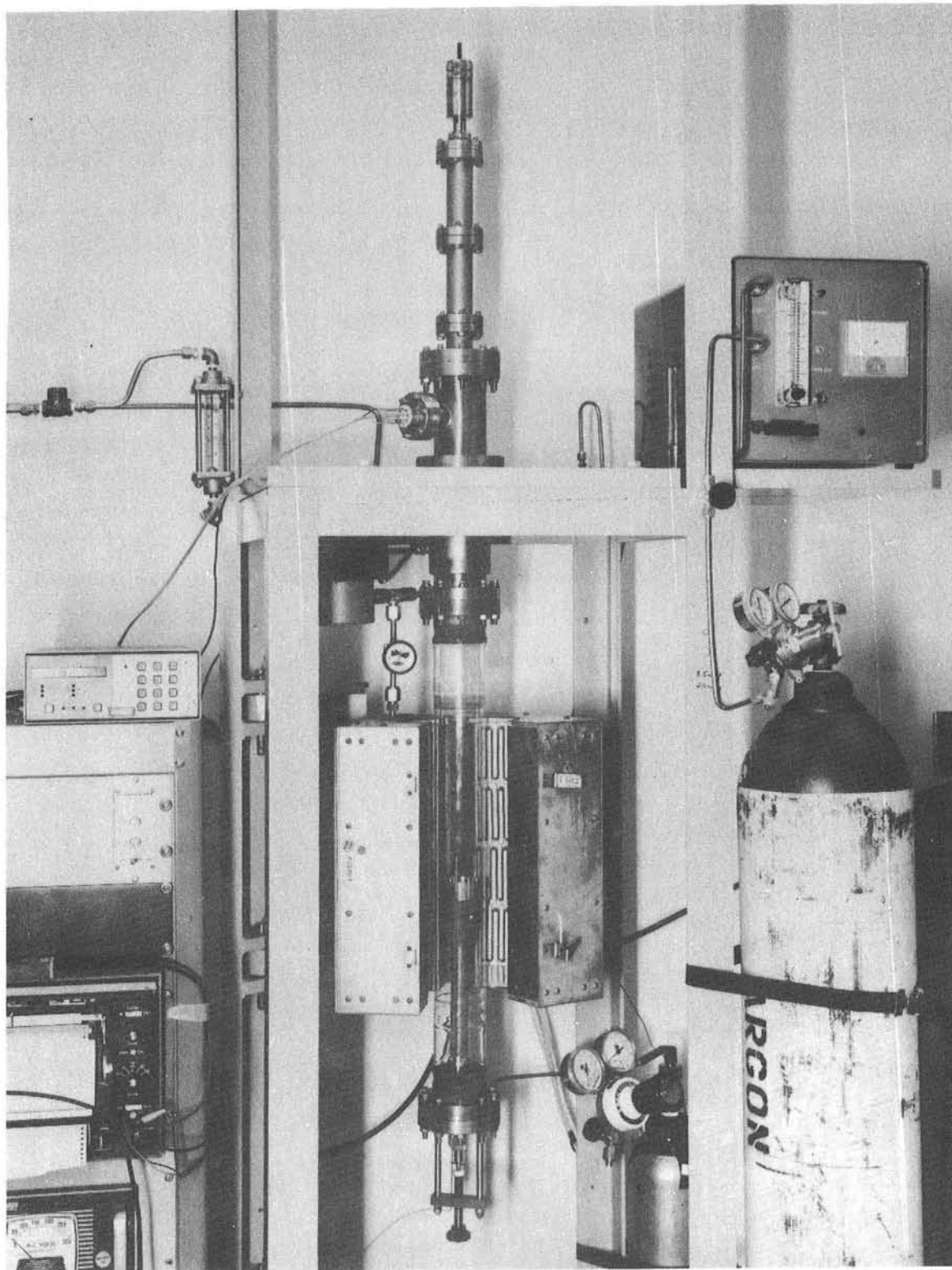


Figure 2. Viscometer Assembly

Figure 3 shows the relationship between the quantity $\sqrt{\eta_p}$ and the experimentally measured values of the logarithmic decrement for these materials. The equation

$$\sqrt{\eta_p} = 70.00 \delta + 0.040$$

was obtained from a least-squares fit of the data. Each data point in Figure 3 is the average of 10 measurements. The average standard deviation is 0.25%.

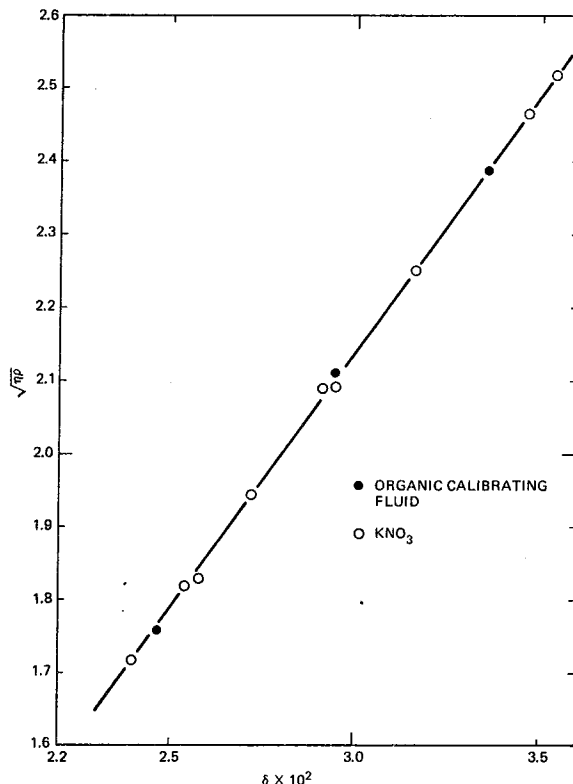


Figure 3. Viscometer Calibration Plot

Surface Tension

In addition to functioning as a viscometer, the apparatus can be converted to an instrument for measuring surface tension with a few minor modifications.¹

By slowly and continuously separating the liquid and the plate immersed in it, and measuring the maximum force exerted on the plate (which occurs just before the column of liquid supported by the plate breaks), one can determine the surface tension of the liquid by the formula

$$\gamma = \frac{F}{P \cos \theta} \quad (4)$$

where γ is the surface tension; F is the maximum force exerted on the plate, which detected as an apparent increase in the weight of the plate; P is the perimeter of the plate; and θ is the wetting angle, generally assumed to be zero if the liquid wets the plate. The gold plate in these experiments was 1.609 cm wide and 0.0262 cm thick.

Density

The apparatus can also function as an Archimedean densitometer.¹ The loss in weight (Δw) of a solid of known volume (V) is related to the density of the liquid (ρ) in which it is immersed by

$$\rho = \frac{\Delta w}{V} . \quad (5)$$

Therefore, the density of a liquid is given simply by the difference in LVDT reading, converted to weight, with and without liquid surrounding the solid, divided by its volume. For increased accuracy of the density measurements the thin plate was replaced by a larger volume bob. The bob presently used is made of gold-plated zirconium and is in the form of a right circular cylinder with a tapered top and bottom to permit drainage. A small post with a hole drilled through it extends from the top taper to provide a means of attaching the bob to the LVDT.

For measurements of density using Archimedes' method it is necessary that the volume of the immersed body be accurately known. This was determined by immersing the bob in several liquids of known density. The volume of the bob was determined to be $1.3518 \pm 0.0005 \text{ cm}^3$.¹

Results and Discussion

The thermophysical properties that we determined for the equimolar $\text{NaNO}_3\text{-KNO}_3$ mixture are presented and discussed in this section. These data cover the range 300-600°C and were taken in argon and in oxygen to determine what effect, if any, the composition of the atmosphere might have. Variations in the oxygen partial pressure will result in changes in the nitrite/nitrate ratio, cf. Eq. (6), which may have an effect on the thermophysical properties, particularly if this ratio becomes large. It was found that, with the exception of the density, the thermophysical properties are unaffected by atmospheric composition. This statement must be treated with some caution, however, since extended exposure of the melt to an argon atmosphere at 600°C will result in the production of increasingly large quantities of nitrite. This is a consequence of the thermal decomposition of nitrate,



So that the dependence of the thermophysical properties on nitrite concentration may be more fully characterized, the MNO_3/MNO_2 system (M being Na or K) is presently being studied in detail.

The $NaNO_3$ and KNO_3 in these experiments were recrystallized from distilled water at least once and vacuum dried at $150^\circ C$ before use. At the conclusion of each experiment the salt was analyzed for its nitrite content. This analysis involved the oxidation of the NO_2 by $Ce(IV)$ and back-titrating with oxalate. A more complete discussion of this method is given in Reference 5.

Where they are available, literature values are compared with our data.

Surface Tension

The surface tension of the equimolar $NaNO_3-KNO_3$ mixture is given in Table I and Figure 4. Over the range $300-600^\circ C$ in both argon and oxygen these data can be satisfactorily represented by the equation

$$\gamma(\text{dynes/cm}) = 133.12 - 6.25 \times 10^{-2}T(\text{ }^\circ\text{C}) \quad (7)$$

with an uncertainty of $\pm 0.5\%$.

TABLE I
SURFACE TENSION OF EQUIMOLAR $NaNO_3-KNO_3$

$T(\text{ }^\circ\text{C})$	γ (Expt) (dynes/cm)	γ (dynes/cm) ⁴	γ (dynes/cm) ⁵
257	117.1	120.0	117.9
267	116.5	119.2	117.0
280	115.6	118.2	115.7
307	114.4	116.3	-
350	111.3	113.0	-
400	108.1	109.7	-
450	105.0	-	-
500	101.7	-	-
547	109.0	-	-
594	96.0	-	-

The excellent agreement between our data and those of Krivovyyazov et al.,⁶ Table I and Figure 4, suggests that the data of Reference 4 are incorrect. The agreement between these two sets of data is particularly reassuring since the data of Krivovyyazov et al. were obtained by a different method, maximum bubble pressure vs. plate detachment. A more complete discussion of this difference is given in Reference 1.

The close agreement between the surface tension values measured in oxygen and argon, Figure 4, implies that the presence of small concentrations of nitrite (< 7 wt%) has little effect on the surface tension of the nitrites.

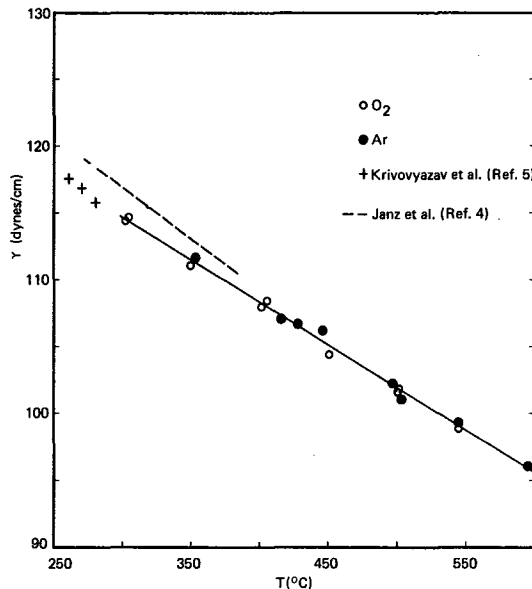


Figure 4. Surface Tension of $\text{NaNO}_3\text{-KNO}_3$ vs Temperature

This result would be expected since the nitrates have a lower surface tension than the corresponding nitrites and thus would tend to concentrate at the surface.⁷

Density

The density of the equimolar $\text{NaNO}_3\text{-KNO}_3$ mixture in argon or oxygen is presented in Table II and Figure 5. The first set of data can be represented by the equation

$$\rho(\text{g/cm}^3) = 2.100 - 6.56 \times 10^{-4}T(\text{°C}) \quad (8)$$

with an uncertainty of $\pm 0.5\%$ from 300-600°C. We have found, however, that if the melt is held for 72 hours at 600°C in an argon atmosphere there is a decrease in the density. The new values of the density are given by

$$\rho' = 2.074 - 6.36 \times 10^{-4}T \quad (9)$$

This decrease in density is attributed to the presence of ≈ 7 wt% nitrite in the melt which results from the thermal decomposition of nitrate, Eq. (6).

TABLE II
DENSITY OF EQUIMOLAR $\text{NaNO}_3\text{-KNO}_3$

$T(^{\circ}\text{C})$	$\rho(\text{Expt}) \text{ (g/cm}^3)$	$\rho^4 \text{ (g/cm}^3)$
298	1.905	1.900*
347	1.873	1.872
400	1.836	1.835
442	1.810	1.805
498	1.774	-
555	1.735	-
595	1.709	-
--- 72 hours at 600°C in argon ---		
607	1.686	-
506	1.757	-
406	1.813	1.831
298	1.877	1.900*

*Extrapolated.

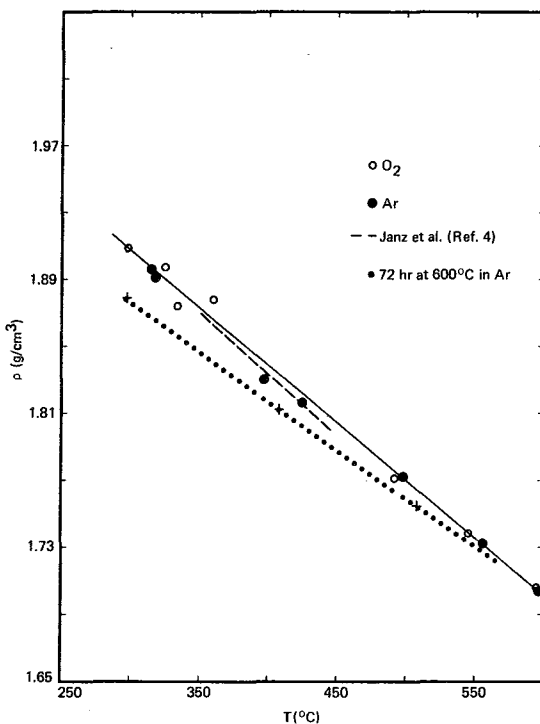


Figure 5. Density of $\text{NaNO}_3\text{-KNO}_3$ vs Temperature

Viscosity

The viscosity of the equimolar $\text{NaNO}_3\text{-KNO}_3$ mixture between 300 and 600°C, in argon and oxygen, is shown in Figure 6. For comparison, values of the viscosity from Reference 4 are included. To facilitate comparison the solid line in Figure 6 is drawn through the literature data. It can be seen that agreement between the two sets of values is quite good. The viscosity may be calculated from the equation

$$\eta(\text{cP}) = 22.714 - 0.120T + 2.281 \times 10^{-4}T^2 - 1.474 \times 10^{-7}T^3,$$

for T in °C, with an uncertainty of 1.0%.

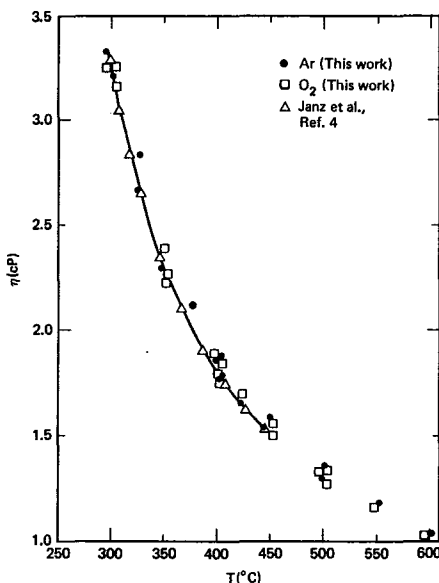


Figure 6. Viscosity of $\text{NaNO}_3\text{-KNO}_3$ vs Temperature

If we make the assumption that for ideal or near-ideal solutions the temperature dependence of the viscosity may be written in the form⁸

$$\eta = \eta_0 \exp(-E_\eta/RT) \quad (10)$$

where E_η is the activation energy for viscous flow and R and T have their usual meanings, then $\ln \eta$ should depend linearly on the reciprocal of the absolute temperature. In Figure 7 our viscosity data and the recommended literature values are plotted as $\ln \eta$ against $1/T$. Rather than a single straight line the data are seen to fall on a smooth curve which is asymptotic to a straight line at both the low and high temperature limits. The change in slope appears to be in the vicinity of 385°C. Above this temperature E_η , calculated from the limiting slope, is 3.2 kcal/mole while below it $E_\eta = 4.6$ kcal/mole.

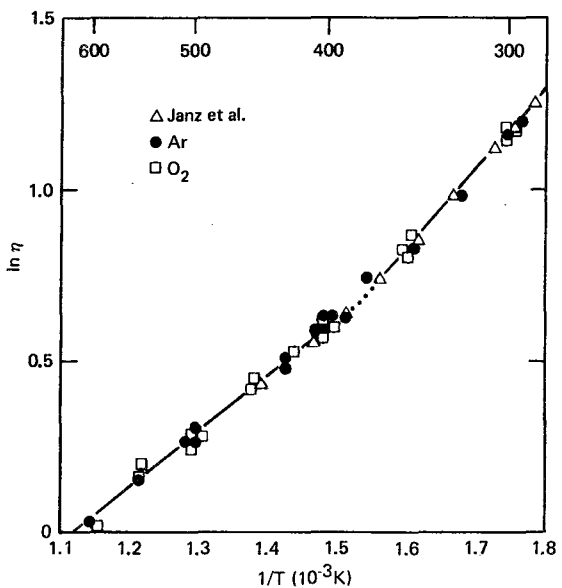


Figure 7. Log Viscosity of $\text{NaNO}_3\text{-KNO}_3$ vs Inverse Temperature

It is possible that the change in slope of this curve at 385°C is caused by the presence of nitrite in the melt arising from the thermal decomposition of nitrate, Eq. (6). However, if this were the case one would expect to see different values of the viscosity in oxygen and argon; this was not observed. A pronounced curvature of that part of the plot above 385°C would also be expected as a consequence of the increased production of nitrite at the higher temperatures; this was also not observed. Therefore, the presence of small amounts of nitrite appears to have negligible effect on the viscosity of nitrate melts.

In general, for low viscosity liquids the temperature dependence of the viscosity is best given by Eq. (10).^{9,10} For a number of liquids, however, behavior similar to that shown in Figure 7 has been observed.⁹ Two examples of this are illustrated in Figure 8 where values of $\ln n$ vs $1/T$ are plotted for methylene iodide (CH_2I_2) and water (H_2O).^{11,12} Spectroscopic evidence suggests that rotation of the CH_2I_2 molecules is restricted because of steric hindrance¹³; hydrogen bonding plays a similar role in H_2O . The conclusion which these data suggest is that in those instances where molecular rotation is restricted because of either steric hindrance or strong intermolecular attraction, e.g., hydrogen bonding, the temperature dependence of the viscosity cannot be adequately described by a single value of E_n . This conclusion has been supported by molecular volume calculations⁹ which show that in those instances where the molecules are free to rotate about at least two axes, Eq. (10) is obeyed over the entire liquid range. However, the onset of non-Arrhenius viscosity behavior occurs at that temperature at which rotation about two axes becomes restricted. That is, a molecule whose rotation is restricted is less able to translate freely than one whose rotation is free, because it is more difficult for the restricted molecule to rotate into a favorable orientation for moving past its neighbors.

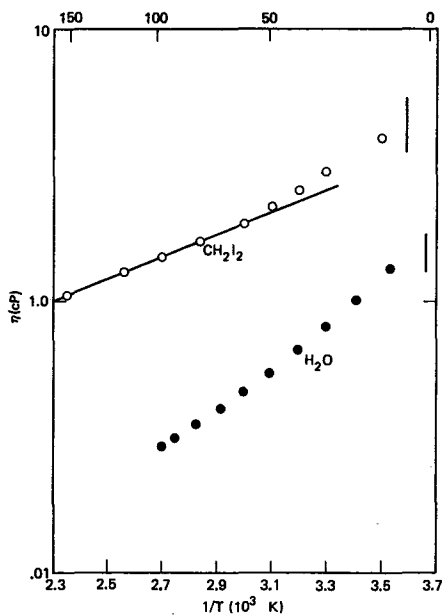


Figure 8. Log Viscosity of CH_2I_2 and H_2O vs Inverse Temperature (Vertical lines designate melting point)

A corollary is that spherical molecules should obey Eq. (10). Figure 9 shows a plot of $\ln \eta$ vs $1/T$ for the equimolar mixture NaCl-KCl ,¹⁴ which is composed of spherically symmetric ions.¹⁵ It can be readily seen that Eq. (10) is obeyed over the entire 170°C temperature range for which data are available (727 - 897°C).

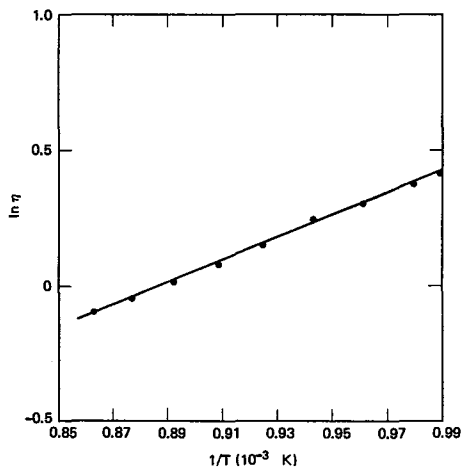


Figure 9. Log Viscosity of NaCl-KCl vs Inverse Temperature

In contrast to the spherically symmetric chloride ion, the nitrate ion is a planar species of finite thickness and a star-shaped symmetry.¹⁶ It is inferred, therefore, that because of the non-spherical symmetry of the nitrate ion, rotation is restricted at temperatures below 385°C, with a consequent increase in E_η .

While the change in activation energy for viscous flow that was observed for NaNO₃-KNO₃ could be satisfactorily explained by postulating changes in the rotational modes of the nitrate with temperature it may also be considered to arise from equivalent processes such as loosening of the melt structure or a change in the molecular packing.

The discontinuity in viscosity observed in the nitrate melt should correspond to a thermodynamic transition of the second or third order,⁹ i.e., $dC_p/dT = 0$ in the former case and $d^2C_p/dT^2 < 0$ or > 0 in the latter. Experiments are now being done to confirm this discontinuity.¹⁷

The transport properties of liquids, particularly those which have a tendency to form glasses, may often be represented by the Vogel-Tamman equation,¹⁹

$$\ln \eta = A + \frac{B}{T - T_0} \quad (8)$$

where A and B are constants and T_0 is the fundamental reference temperature for transport processes in liquid. It is the ideal-glass transition temperature and represents the lower temperature limit of the fluidlike regime. That is, at this temperature the viscosity becomes infinite for the equimolar NaNO₃-KNO₃ mixture. A fit to our viscosity data could only be obtained for $T_0 > 200^\circ\text{C}$, which is only 25°C below the liquidus temperature. For comparison, Moynihan¹⁹ has estimated that the glass transition temperature for KNO₃ is 5°C.

Summary

We have determined the viscosity, surface tension, and density for the equimolar mixture NaNO₃-KNO₃ in both argon and oxygen. Both the surface tension and viscosity of this salt mixture are unaffected by small concentrations of nitrite (≈ 7 wt%), formed by thermal decomposition of nitrate in an argon atmosphere, while the density was lowered slightly. The viscosity showed a change in activation energy at 385°C, which was attributed to a freeing of one of the rotational modes of the nitrate ion as the temperature increased above this value.

REFERENCES

1. D. A. Nissen, "A Single Apparatus for the Precise Measurement of the Physical Properties of Liquid at Elevated Temperature and Pressure," SAND80-8034, October 1980.
2. C. R. Wylie, Advanced Engineering Math. (McGraw-Hill Book Co., New York, 1960), p. 205.
3. C. Solomons and M. S. White, Trans. Faraday Soc. 65, 305 (1969).
4. G. J. Janz, U. Krebs, H. E. Siegenthaler, and R. P. T. Tomkins, J. Phys. & Chem. Ref. Data 1, 587 (1972).
5. D. A. Nissen & D. E. Meeker, to be published.
6. E. L. Krivovyazov, I. D. Sokolova, and H. K. Voskresenskaya, Russ. J. Appl. Chem., 36, 2458 (1963).
7. H. Bloom, F. G. Davis & D. W. James, Trans. Faraday Soc. 56, 1179 (1960).
8. W. Brockner, K. Tørklep and H. A. Øye, Ber. Bunsenges. Phys. Chem. 83, 12 (1979).
9. D. B. Davies and J. Matheson, J. Chem. Phys. 45, 1000 (1966).
10. D. Dumas, B. Fjeld, K. Grotheim, and H. A. Øye, Acta. Chem. Scand. 27, 31a (1973).
11. J. Timmermans, Physico-Chemical Constants of Pure Organic Compounds (Elsevier, New York, 1950).
12. Handbook of Chemistry & Physics, 26th edition, edited by C. D. Hodgman, (Chemical Rubber Co., Cleveland, Ohio, 1942), p. 1638.
13. W. J. Jones, and H. Sheppard, Report Conf. Hydrocarbon Research Group (Inst. of Petroleum, London, 1962), p. 181.
14. G. J. Janz, R. P. T. Tomkins, C. B. Allen, J. R. Downey, G. L. Gardner, U. Krebs, and S. K. Singer, J. Phys. & Chemical Ref. Data 4, 871 (1975).
15. A. Timedei and G. J. Janz, Trans. Faraday Soc. 64, 202 (1968).
16. G. J. Janz and D. W. James, J. Chem. Phys. 35, 739 (1961).

17. R. W. Carling, Sandia National Laboratories, Livermore, CA, private communication.
18. A. R. Ubbelohde, The Molten State of Matter, (John Wiley & Sons, New York, 1978), p. 361.
19. C. T. Moynihan in Ionic Interactions, edited by S. Petrucci (Academic Press, New York, 1971), Vol. 1, p. 274.

UNLIMITED RELEASE
INITIAL DISTRIBUTION

Division of Solar Technology
U.S. Department of Energy
Washington, D.C. 20545
Attn: W. Auer
G. W. Braun
M. U. Gutstein
J. E. Rannels

U.S. Department of Energy/STOR
Washington, D.C. 20545
Attn: J. H. Swisher
J. Gahimer

D. Krenz
Special Programs Office
Albuquerque Operations Office
U.S. Department of Energy
P. O. Box 5400
Albuquerque, New Mexico 87115

R. Hughey
San Francisco Operations Office
U.S. Department of Energy
1333 Broadway
Oakland, California 94612

C. A. Bolthrunis
Badger Energy, Inc.
One Broadway
Cambridge, Massachusetts 02142

D. L. Erickson
Energy Concepts Company
627 Ridgely
Annapolis, Maryland 21401

JPL
4800 Oak Grove Drive
Pasadena, California 91103
Attn: J. Becker
R. Manvi
V. Truscello

Martin Marietta Corp.
P. O. Box 179
Denver, CO 80118
Attn: D. Beshore
T. R. Tracey

McDonnell Douglas Astronautics Company
5301 Bolsa Avenue
Huntington Beach, California 92647
Attn: C. R. Easton
D. L. Endicott

Solar Energy Research Institute
1536 Cole Boulevard
Golden, CO 80201
Attn: B. Butler
B. Gupta
K. Touryan
C. Wyman

Dr. M. Taube
Swiss Federal Institute
for Reactor Research
CH-5305 Wurenlingen
Switzerland

Prof. H. A. Øye
c/o F. J. Seiler Research Lab
(AFSC) USAF Academy
Colorado 80840

Dr. B. Hafskjold
Institutt for Uorganisk Kjemi
Norges Tekniske Høgskole
Universitetet i Trondheim
H-7034 Trondheim-NTH, Norway

R. S. Claassen, 5800; Attn: R. G. Kepler, 5810
R. E. Whan, 5820
J. H. Sweet, 5824
M. J. Davis, 8530
N. J. Magnani, 5840

T. B. Cook, 8000; Attn: A. N. Blackwell, 8200
L. Gutierrez, 8400

B. F. Murphey, 8300; Attn: R. L. Rinne, 8320
G. W. Anderson, 8330
W. Bauer, 8340
D. L. Hartley, 8350

D. M. Schuster, 8310

W. R. Hoover, 8312

R. W. Mar, 8313

D. A. Nissen, 8313 (15)

A. J. West, 8314

L. A. West, 8315

J. C. Swearengen, 8316

R. C. Wayne, 8450; Attn: W. G. Wilson, 8453

R. W. Carling, 8453

L. G. Radosevich, 8453

Publications Division, 8265, for TIC (27)

Publications Division, 8265/Technical Library Processes and Systems Division, 3141

Technical Library Processes and Systems Division, 3141 (2)

Library and Security Classification Division, 8266 (3)